

Research Paper

Membrane-Assisted Photocatalytic Degradation of Perfluorooctanoic Acid

Inmaculada Ortiz*, Laura Rancaño, Maria J. Rivero, Ane Urriaga

Departamento de Ingenierías Química y Biomolecular, Universidad de Cantabria, Av. Los Castros s/n, 39005, Santander, Spain

Article info

Received 2023-03-14

Revised 2023-03-24

Accepted 2023-03-28

Available online 2023-03-28

Keywords

Perfluorooctanoic acid

Composite photocatalysis

TiO₂ P25

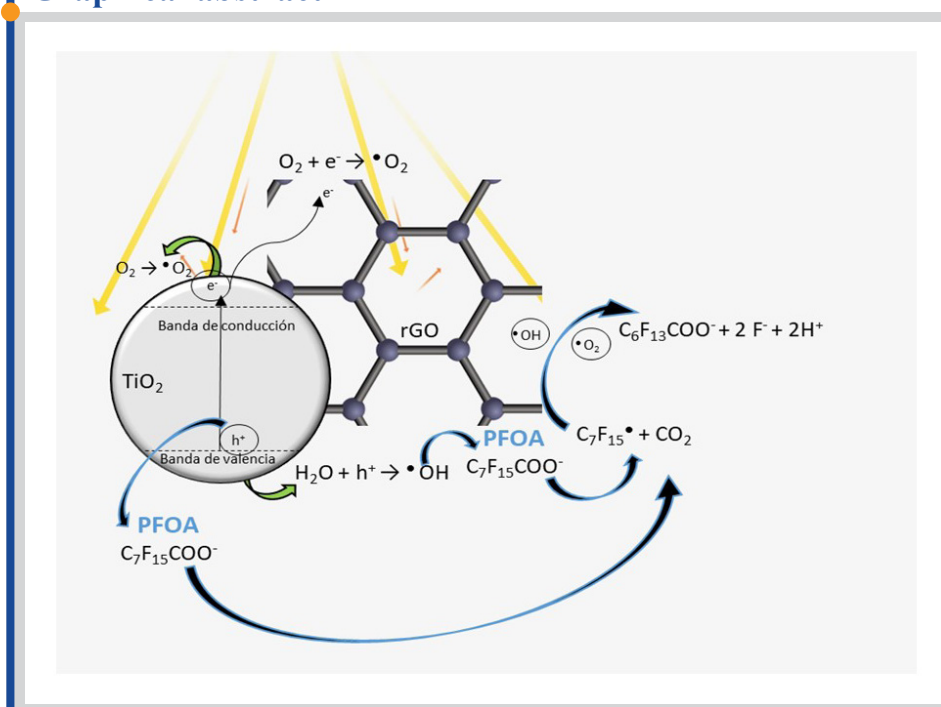
Reduced graphene oxide

Reverse osmosis pre-treatment

Highlights

- Improvement of the perfluorooctanoic acid (PFOA) degradation.
- Analysis of the photocatalyst performance and influence of the operating variables.
- Benefits of a membrane concentration step before the photocatalytic oxidation.

Graphical abstract



Abstract

The ubiquitous presence of per- and poly-fluoroalkyl substances (PFAS) in the environment together with their persistence urges the development of cost-effective remediation technologies to be applied to their aqueous sources thus, preventing their entrance to nature. Among all PFAS, perfluorooctanoic acid (PFOA) has been identified as a substance of very high concern due to its extreme persistence, bioaccumulation, and mobility in the environment; however, conventional technologies for water remediation report low yield in PFOA degradation. Photocatalytic degradation reports outstanding characteristics in its application to the degradation of recalcitrant compounds. This alternative relies on the properties and characteristics of the semiconductor material used as a photocatalyst, a fact that has prompted a series of works related to the synthesis and viability of new catalysts in recent years. After the preliminary results obtained in our group with a new composite photocatalyst based on the combination of the more extended TiO₂ P25 semiconductor with reduced graphene oxide, TiO₂-rGO 5%, this work provides a deeper analysis of the influence of operation conditions on the degradation kinetics and highlights the relevance of a membrane pre-concentration step, especially for the removal of aqueous matrixes with low PFOA concentration.

© 2023 FIMTEC & MPRL. All rights reserved.

1. Introduction

Per- and poly-fluoroalkyl substances (PFASs) are synthetic chemical compounds, which are introduced to the environment through their manufacturing and use in industry and consumer products, with applications as surfactants, coatings, water repellents for leather and textiles, in metal plating and aqueous film-forming foam used in firefighting, among others [1,2]. The term PFAS represents a large and diverse set of substances; the US Environmental Protection Agency has a list of more than 7000 PFAS [3]. Among all PFAS, perfluorooctanoic acid (PFOA) is identified as a substance

of very high concern due to its extreme persistence, bioaccumulation, and mobility in the environment. While there is no direct evidence linking PFAS exposure to human deaths, there are numerous studies suggesting that PFAS exposure may be connected to several adverse effects on human health [4,5]. Therefore, PFOA was included in Annex A of the Stockholm Convention on Persistent Organic Pollutants (POPs), meaning that signing parties are committed to taking measures to eliminate its production and use [6]. Health concerns prompted manufacturers in Europe and North America to phase out

* Corresponding author: ortizi@unican.es (I. Ortiz)

the production of PFOA, although the decline has been offset by the increase in other regions such as Asia [7,8]. Moreover, the legacy of previous use of PFOA remains in landfill leachates [9], effluents of wastewater treatment plants [10], and groundwater impacted by aqueous film forming foams contaminated soils [11]. The USEPA established health advisory levels (HALs) for perfluorooctanoic acid (PFOA) and perfluorooctane sulfonate (PFOS) in drinking water at 0.07 µg/L, both individually and combined [12]. Likewise, the European Directive on the quality of water intended for human consumption encourages member states to limit the sum of PFAS in drinking water below 0.10 µg/L [13]. Meanwhile, a report documented that up to 6 million U.S. residents might be exposed to drinking water that exceeds these HALs [11].

Many studies emphasize the low efficiency of conventional water treatment technologies for the elimination of PFOA [14,15]. A recently published study reports an intensive survey of PFOA and PFOS concentrations in the effluents of numerous wastewater treatment facilities in the United Kingdom [16]. Furthermore, this study concluded that PFOA concentration in the effluent was on a whole increasing up to 35%, compared to influent concentration. Other studies on the removal of PFOA during wastewater treatment demonstrate that effluent concentrations can be higher than influent levels owing to its formation via the biodegradation of precursor compounds [17,18].

Adsorption and ion exchange are the most extensively studied technologies for PFAS removal from water. However, adsorption techniques have several disadvantages, such as the low efficiency of regeneration of adsorbents, and when applicable, the generation of large amounts of waste organic solvents used as regenerants [19]. A different approach for separating PFAS from water is to apply nanofiltration and reverse osmosis membrane processes [20-24]. Combining membrane separation with efficient degradation technologies such as electrocatalysis or electrooxidation to degrade the PFAS retained in the concentrate has been explored as a more efficient treatment than oxidation alone [25,26].

PFOA photocatalytic decomposition, with the advantage of low energy consumption, requires highly efficient photocatalysts able to perform PFOA degradation at mild conditions. Although TiO₂ shows a limited performance for PFOA degradation, an increasing number of semiconductors, such as materials based on In, Ga and Bi have shown much higher effectiveness in PFOA degradation [27-29]. Notably, TiO₂ properties for the degradation of perfluorochemicals have been improved by hybridizing them with carbonaceous materials such as carbon nanotubes [30] and graphene nanosheets [31]. One approach consists of the concentrate and destroys strategy, in which the activated carbon adsorbs and concentrates the contaminant on the photoactive sites, facilitating the subsequent degradation of PFOA [32-34]. Graphene-related materials, e.g., reduced graphene oxide (rGO), possess excellent properties such as high electrical conductivity and electron mobility. The electronic properties of rGO decrease the electron-hole recombination rate in the TiO₂, as well as reduce the nano-composite band-gap and contribute to avoiding the agglomeration of the nanoparticles which is usually found for TiO₂ P25 catalyst [35-37]. Pachangam et al. [38] and Shang et al. [39] reported the photocatalytic degradation of PFOA on Pb-BiFeO₃/rGO catalyst under UV 254 light achieving 69.6% PFOA degradation and 28% mineralization under the optimal conditions. Gomez-Ruiz et al. [35] reported that low dosages (0.05 g/L) of TiO₂-rGO under UV-Vis light achieved 93±7% PFOA removal and 62% mineralization after 12 hours, a notable enhancement compared to TiO₂ that in the same operation conditions only degraded 24% of PFOA. Using graphene oxide deposited TiO₂ nanotube arrays PFOA degradation was favored at acidic pH [40], although the authors concluded that PFOA degradation efficiency was strongly dependent on operational parameters, on which the information was still insufficient. Within this context and considering the promising results so far obtained with composite photocatalysts containing graphene oxide (and its reduced form) this work deepens the influence of the operation variables, namely, solution pH and concentration of PFOA on the degradation kinetics highlighting the potential improvement of membrane concentration before the photocatalytic oxidation, especially for low concentrations such as those found in contaminated waters.

2. Materials and methods

2.1. Chemicals

Perfluorooctanoic acid (C₇F₁₅COOH) and p-benzoquinone (BQ) were obtained from Sigma-Aldrich. Graphene oxide (GO) water dispersion of 0.4 wt% was acquired from Graphenea and titanium dioxide TiO₂ Aeroxide P25 was purchased from Evonik Industries. Sodium hydroxide 50% solution was obtained from EMSURE and hydrochloric acid 0.1 mol/L, and formic acid 85%

(FA) from PanReac. Ammonium acetate and UHPLC-MS grade methanol from Scharlab were used for analytical purposes. Tert-butanol (t-BuOH) was obtained from Sigma-Aldrich.

2.2. Synthesis and characterization of TiO₂-rGO photocatalyst

The photocatalyst was composed of 95 wt% of TiO₂ P25 and 5 wt% of reduced graphene oxide synthesized by the hydrothermal method [35,41-45]. In summary, 150 mL of ultrapure water containing 760 mg of commercial TiO₂ was mixed with 10 mL of the GO commercial solution. These conditions were selected from previous studies of the research group [36,37]. After stirring for 2 h, the solution was introduced in a 200 mL Teflon-lined stainless-steel autoclave and maintained at 120 °C for 3 h to achieve the GO reduction and the loading of the titanium dioxide on the reduced GO sheets. Finally, the composite was centrifuged, rinsed with ultrapure water, and fully dried at 50 °C overnight.

Fourier-transform infrared (FT-IR) spectra of the synthesized TiO₂-rGO composite were determined in a Perkin-Elmer equipment. GO samples were dried at 30 °C for 12 h before analysis. Thermal characterization was carried out in a Shimadzu DTG-60H Differential Thermal Gravimetric Analyzer working under a nitrogen atmosphere, with a flowrate of 50 mL/min in the temperature range of 10-500 °C at an increasing rate of 10 °C/min. Moreover, the Zeta potential and the particle size of the photocatalyst were measured in a Zetasizer Nano ZS apparatus (Malvern). Additional characterization of TiO₂-rGO 5% can be found in the literature [36].

2.3. Experimental methodology

All photocatalytic experiments were carried out in a Light Emitting Diodes (LEDs) photoreactor. This light source was used by other research groups [46-48]. A 1 L Pyrex glass vessel was filled with the target solution. LED Enging LZ1-00UV00 light source consisted of 30 units with an emission wavelength of 365 nm; it was placed around the reaction vessel at a 3 cm distance from the reactor wall [49]. Ochiai et al. [50] also treated perfluorocarboxylic acids with UV-A light. The irradiance was 213.4 mW/cm², which corresponded to an electrical power consumption of 75 W. Furthermore, the photocatalytic LEDs reactor included a control panel to set the electrical power consumption and the radiation intensity.

PFOA solutions were prepared using ultrapure water (Q-POD Millipore) with four different initial concentrations of PFOA: 0.12 mM, 0.24 mM, 0.36 mM, and 0.48 mM. Samples of the reaction mixture were extracted at defined time intervals and filtered through a 0.22 µm polypropylene filter (FILTER-LAB) before analysis.

2.4. Analytical techniques

The concentration of PFOA and its degradation products perfluoroheptanoic acid (PFHpA), perfluorohexanoic acid (PFHxA), perfluoropentanoic acid (PFPeA), and perfluorobutanoic acid (PFBA) were analyzed using an ultraperformance liquid chromatography (UHPLC) system (Acquity H-Class, Waters) equipped with an X Bridge C18 column (5 µm, 250 mm x 4.6 mm, Waters) and a triple-quadrupole mass spectrometer (Acquity TQD, Waters). A mixture of methanol (65 %) and dihydrogen phosphate (35 %) was used as the mobile phase in isocratic mode with a flow rate of 0.5 mL/min. The Limit of Quantification (LOQ) was 0.1 µg/L for PFOA and its intermediates. A TOC-V CPH (Shimadzu) was used to quantify Dissolved Organic Carbon (DOC). Finally, the fluoride ions concentrations were measured in an ICS-1100 (Dionex) ion chromatograph equipped with an AS9-HC column in isocratic mode using Na₂CO₃ 9 mM as eluent with a flow rate of 1 mL/min, and a pressure of approximately 2000 psi, based on Standard Methods 4110B [51].

3. Results

3.1. Characterization of TiO₂-rGO 5% composite photocatalyst

Fig. 1a shows the FT-IR spectra of the commercial titanium dioxide, reduced graphene oxide, and the synthesized composite TiO₂-rGO 5%, assessing the successful synthesis of the composite as reported elsewhere [36,52] and Fig. 1b shows the FT-IR spectra of the catalyst after the degradation experiments. Bands assigned to C-F stretching can be found in the range 1300-1100 cm⁻¹ [32,53]. The increase in the intensity of these bands may point to the amount of adsorbed fluorinated compounds onto the catalyst during the photocatalytic treatment.

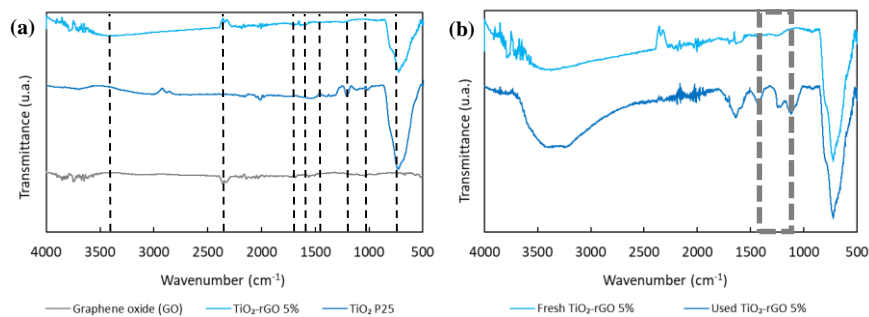


Fig. 1. a) FT-IR spectra of the catalyst before and b) after the photodegradation experiment. $[PFOA]_0 = 0.36$ mM, $[TiO_2\text{-rGO } 5\%] = 0.05$ g/L, pH = 2.5.

Fig. 2 shows the change of Zeta potential with pH for TiO_2 P25 and $TiO_2\text{-rGO } 5\%$ composite. The point of zero charge (ZPC) of the composite takes a value of 5.2, lower than the ZPC corresponding to TiO_2 P25, 6.25. Thus, both TiO_2 and $TiO_2\text{-rGO } 5\%$ catalysts reported a positive surface charge for pH values lower than the corresponding ZPC. Finally, the particle size was measured for the two photocatalysts leading to average values of 763 ± 30 nm for TiO_2 P25 and 1288 ± 40 nm for the $TiO_2\text{-rGO } 5\%$ composite, respectively. This increase in the particle size of the composite is in agreement with the literature data [54].

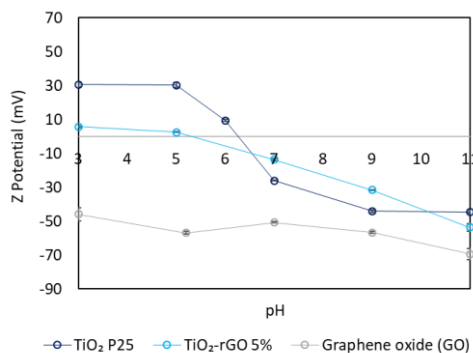


Fig. 2. Zeta potential for TiO_2 P25, graphene oxide (GO), and $TiO_2\text{-rGO } 5\%$.

3.2. PFOA photocatalytic degradation

Initially and to compare the activity of the two catalysts, preliminary degradation runs of PFOA were carried out with no pH control starting with initial PFOA concentrations between 0.12 mM (pH = 4.32 ± 0.17) and 0.48 mM (pH = 3.53 ± 0.07). Figs. 3 and 4 depict the kinetic trends of PFOA disappearance and the formed intermediate compounds.

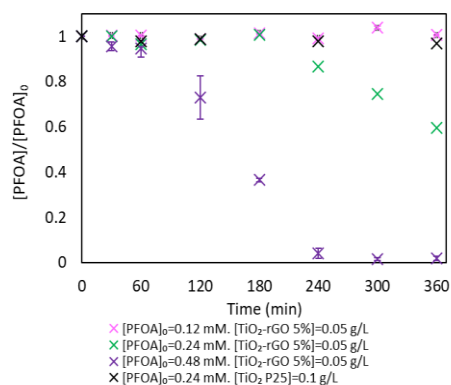


Fig. 3. Photocatalytic degradation of PFOA at natural pH.

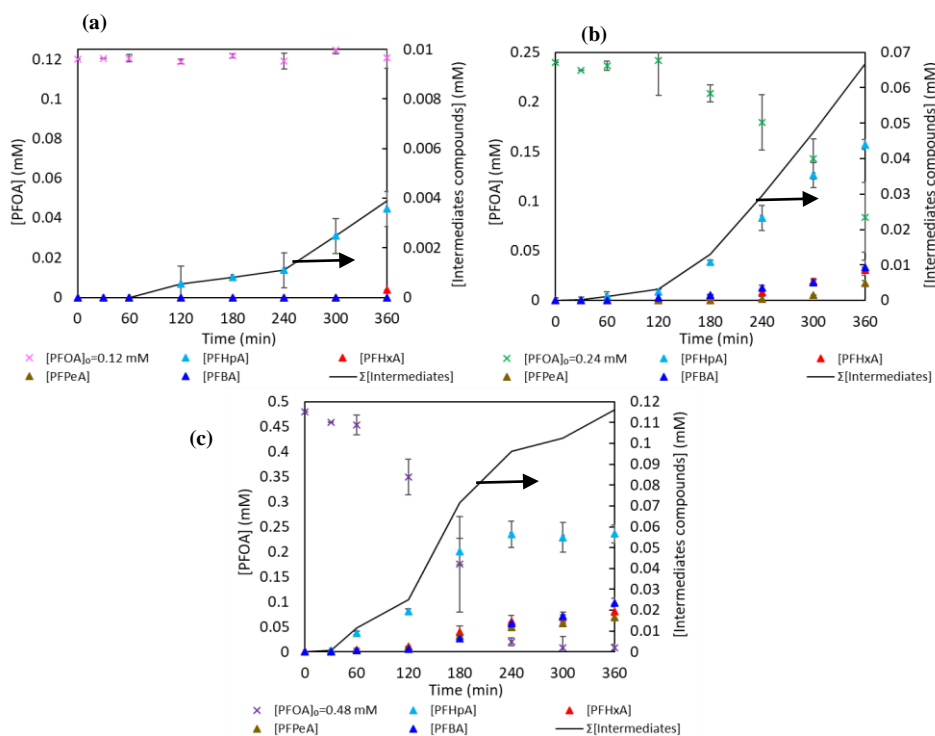


Fig. 4. Intermediate acidic derivatives for the experiments at natural pH for a) $[PFOA]_0 = 0.12$ mM, b) $[PFOA]_0 = 0.24$ mM, c) $[PFOA]_0 = 0.48$ mM. $[TiO_2\text{-rGO } 5\%] = 0.05$ g/L, irradiance = 213.4 mW/cm^2 .

After these experiments, it was concluded first, that the composite is more effective in the degradation of PFOA than TiO₂ P25 and second, that the higher the initial concentration of the acid the higher the degradation rate. The kinetic trend followed with the initial concentration of PFOA is, however, highly surprising and contrary to that observed in previous works for different initial concentrations [53,55]. Sansotera et al. [53] showed that the fastest PFOA degradation was achieved for the lowest concentration in the range between 4.0 mM and 12.0 mM, although pH control was not reported. To shed light on this behavior the possible effect of the pH in the starting solutions was considered. At first, the increase of the acidity of the solution with an increasing initial concentration of PFOA was associated with a higher degradation rate. Next, a set of experiments working under controlled pH of 2.5 that was kept constant by adding hydrochloric acid was carried out.

Fig. 5a shows the kinetic curves corresponding to four different initial concentrations of PFOA whereas Fig. 5b shows the comparison of the

performance of the composite and the individual components for an initial concentration of PFOA of 0.36 mM. Before the experiments, the adsorption of the pollutant on the catalyst was assessed. Dark adsorption was negligible and so was photolysis without a catalyst. The adsorption of PFOA onto TiO₂ was also reported to be insignificant in the literature [56,57].

Wang et al. [27], in a critical review of the photocatalytic degradation of PFOA, discussed the influence of pH and summarised that PFOA photodegradation with TiO₂ was more favorable in an acidic solution because the acid would exist as the perfluorooctanoate anion (C₇F₁₅COO⁻) when the solution pH is higher than the pK_a value of PFOA (the authors considered a widely reported value of pK_a = 2.8), therefore when operating in a pH range from 2.8 to 6.25 (point of zero charge for the reported catalyst), the adsorption of C₇F₁₅COO⁻ anions on the TiO₂ surface would be accelerated due to the electrostatic force between C₇F₁₅COO⁻ and the positively charged surface of the catalyst.

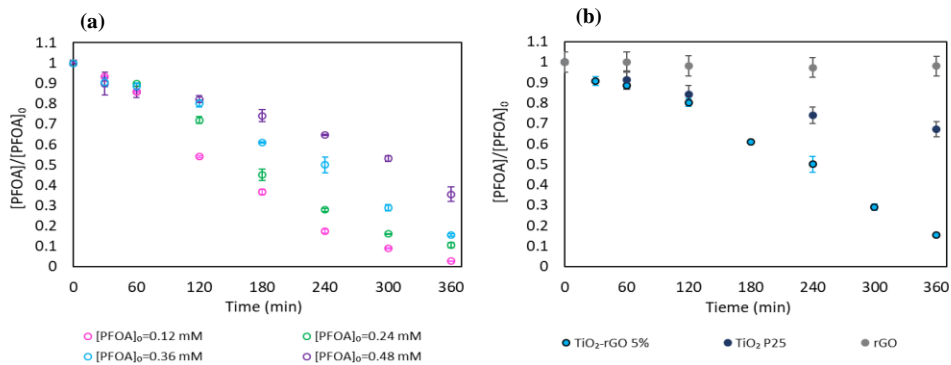


Fig. 5. a) Influence of the initial PFOA concentration on the photocatalytic degradation at pH 2.5, [TiO₂-rGO 5%] = 0.05 g/L, irradiance = 213.4 mW/cm². b) Photocatalytic activity of titanium dioxide, reduced graphene oxide (rGO), and TiO₂-rGO 5% for the PFOA degradation at pH 2.5, [PFOA]₀ = 0.36 mM, [TiO₂-rGO 5%] = 0.05 g/L, [TiO₂ P25] = 0.05 g/L, and [rGO] = 0.0025 g/L, irradiance = 213.4 mW/cm².

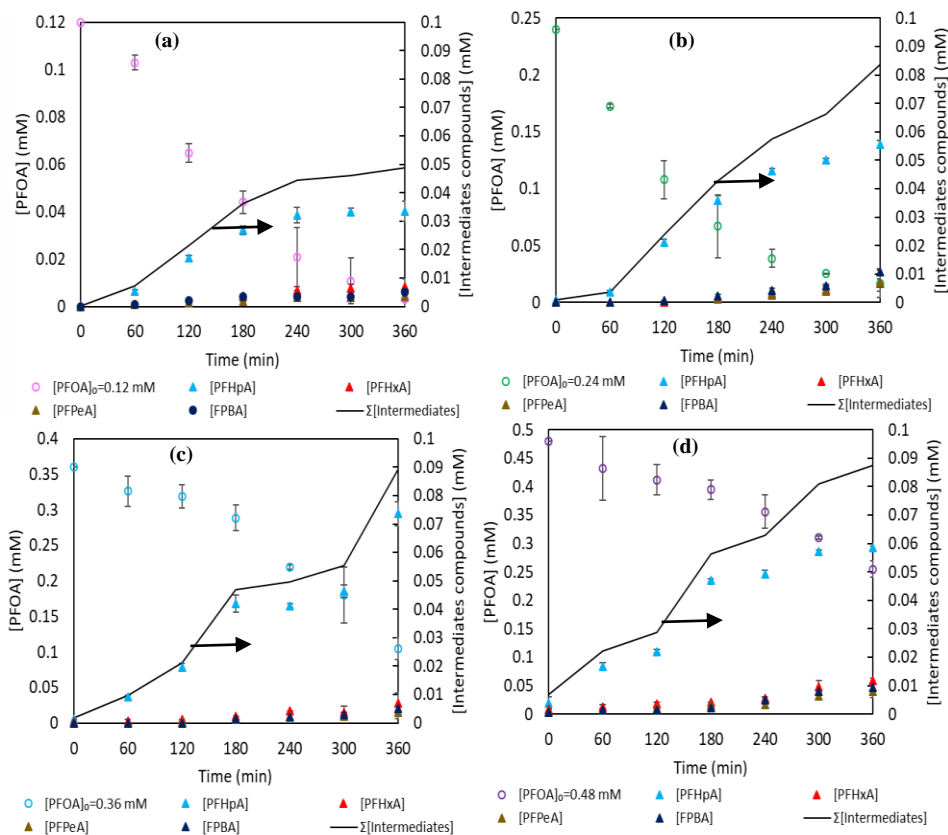


Fig. 6. Intermediate PFCA derivatives for the experiments at pH 2.5 for a) [PFOA]₀ = 0.12 mM, b) [PFOA]₀ = 0.24 mM, c) [PFOA]₀ = 0.36 mM, and d) [PFOA]₀ = 0.48 mM. [TiO₂-rGO 5%] = 0.05 g/L, irradiance = 213.4 mW/cm².

More recently, Xu et al. [58] in experiments of PFOA degradation by TiO_2 and peroxymonosulfate working in the pH range $3.0 \leq \text{pH} \leq 9.0$ arrived at similar conclusions, highlighting that the fastest degradation kinetics was achieved in the region of pH between the value of pK_a and the pH of ZPC of the catalyst, 2.8 and 5.6 respectively, according to the authors [39,59]. Thus, it has been repeatedly reported the relevance of the electrostatic attraction between the perfluorooctanoate anions and the positively charged catalyst surface on the degradation kinetics, and this manifests in the pH region between the pK_a of the acid and pH at the ZPC of the catalyst. Determination of the pK_a for these acids has been a subject of great interest in the scientific literature, where values ranging between $\text{pK}_a = 0.5$ [60] to $\text{pK}_a < 1.3$ [61,62] have been most widely reported and explained. Higher pK_a values for PFOA, $\text{pK}_a = 2.8$ and $\text{pK}_a = 3.8 \pm 0.1$ have been reported as well and attributed to i) the presence of the organic solvent, methanol, in the experimental systems, ii) the aggregation of perfluorooctanoate, $\text{CF}_3(\text{CF}_2)_6\text{COO}^-$ anion, in solution, and the formation of a stable $(\text{PFO})_2\text{H}^+$ cluster [62]. Interestingly, Burns et al. [63] reported that the degree of perfluorooctanoate aggregation is concentration dependent, such that pK_a suppression may be directly related to the concentration profile of perfluorooctanoate aggregation. After these works, it is derived that the lower the concentration the weaker the acid character of PFOA; this could partially explain the results of Fig. 3 obtained when no pH control is exerted. However, the results shown in Fig. 5 are barely explained by the influence of the electrostatic attraction between the catalyst surface and the anions in the solution, so the influence of pH in different phenomena involved in photocatalytic degradation must be considered.

Explanations, in addition to the electrostatic forces, have been given in works that reported a positive influence of the solution acidity on the kinetics

of PFOA degradation for different catalysts. Dilliert et al. [57] investigated the photocatalytic removal of 4.4 mM heptafluorobutanoic acid (HFBA) with 2 g/L of TiO_2 using a mercury lamp emitting in the range of 310 - 400 nm. Several concentrations of HClO_4 were added to the medium reaching pH values of 1.9 and 1.0, and observing a faster degradation as pH decreases. The authors attributed this behavior, partially to the influence of pH on the adsorption of the acid on the catalyst surface, on the formation of surface complexes, and the oxidative power of the photocatalyst. Moreover, it was remarked that the oxidative power of the valence band holes in TiO_2 is also pH-dependent and increases as pH decreases. Panchangam et al. [56] studied the decomposition of perfluorooctanoic acid (PFOA), perfluorononanoic acid (PFNA), and perfluorodecanoic acid (PFDA) by heterogeneous photocatalysis with TiO_2 in acidic aqueous solutions. In this case, 60 μM of initial concentration of PFOA and 2 g/L of catalyst, and a low-pressure mercury lamp emitting at 254 nm were used. With 0.15 M HClO_4 68% of PFOA removal was reached after 24 h, and using 0.225 M of HClO_4 , PFOA was below the detection limit after 7 h. This behavior was explained as associated with the influence of the presence of perchloric acid on the ionization of perfluorocarboxylic acids (PFCAs) that favors the electron transfer from the perfluorocarboxylate anion to the hole of the TiO_2 catalyst. Moreover, the authors reported that the acid contributed positively to increasing the operating life of the photogenerated holes. Song et al. [30] with a 365 nm lamp, 30 mg/L of PFOA, and 1.6 g/L of TiO_2 -MWCNT using HCl to acidify the solution to pH 2.0 and NH_3 to reach pH 11.0, observed that at pH 2.0 PFOA was almost completely removed after 8 h meanwhile in alkaline conditions only 58% of PFOA was degraded for the same time. In this case, the positive effect was explained because acidic conditions favor the formation of HO_2^* radical, which is a precursor of H_2O_2 and HO^* .

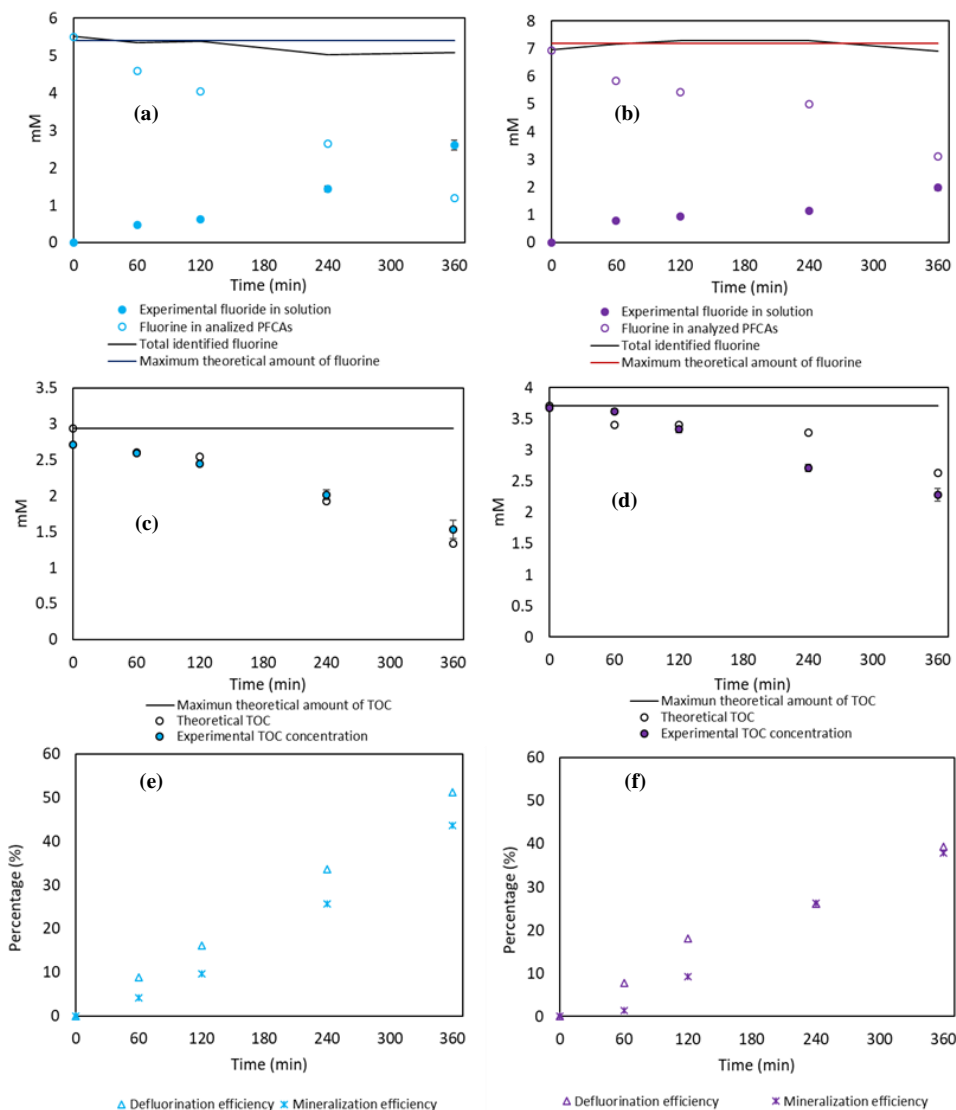


Fig. 7. Fluoride release for the experiments at pH 2.5 for a) $[\text{PFOA}]_0 = 0.36$ mM, and b) $[\text{PFOA}]_0 = 0.48$ mM. TOC for c) $[\text{PFOA}]_0 = 0.36$ mM, and d) $[\text{PFOA}]_0 = 0.48$ mM. Defluorination and mineralization efficiency during the photocatalytic experiments for e) $[\text{PFOA}]_0 = 0.36$ mM, and f) $[\text{PFOA}]_0 = 0.48$ mM. $[\text{TiO}_2\text{-rGO } 5\%] = 0.05$ g/L.

All in all, in this work it has been proved that working at acidic pH (2.5) improves the degradation kinetics. The optimum pH value can be obtained from the dissociation of PFOA when the solubilized concentration is high enough or by the addition of an extra acidic compound. In the literature, interesting works of membrane concentration applied to short-chain perfluorocarboxylic acids or perfluoroalkyl acids can be found with information on the comparative performance of reverse osmosis and nanofiltration membranes [23,24]. The reverse osmosis RO BW30 has reported high rejection percentages of PFOA offering an interesting and clean technology to be applied as pre-treatment of the photocatalytic degradation with the benefit of increasing the concentration of the acid in the treated solution (lowering the pH) and increasing the driving force in the oxidation stage [26].

With regard to the formation of intermediate acidic derivatives, Figs. 4 and 6, depict the results with no pH control and controlled pH, respectively. In all cases it is observed that the total concentration of intermediate compounds is strongly related to the degradation percentage of PFOA and the perfluoroheptanoic acid (PFHpA) is the major intermediate compound showing an increasing trend during the time of the experiments [35,37].

When the PFOA molecule is broken, fluoride ions are released into the solution. Fig. 7 shows the measured fluoride in solution, and the mass balance to fluorine accounting for the measured fluoride and the fluorine content of the organic acids for two different initial concentrations of PFOA. There is a good match between the theoretical and the measured F concentration. The mineralization of the parent compound for the experiments with an initial concentration of PFOA of 0.36 mM and 0.48 mM is also presented in Figs. 7c and 7d, respectively. The theoretical TOC was calculated considering the C atoms in all the quantified compounds, and the experimental TOC is the value measured in the treated solution. It is observed that for both cases, the theoretical TOC concentrations and the experimental measurements are very close. Slight differences could be attributed to experimental errors. Additionally, the defluorination efficiency expressed as (moles of fluoride formed)/(moles of fluorine in initial PFOA), and the mineralization efficiency calculated as (moles of COT measured in solution)/(moles of COT correspondent to initial PFOA concentration) are also presented in Figs. 7e and 7f for the initial concentrations of PFOA of 0.36 mM and 0.48 mM respectively.

4. Conclusions

The promising prospects of photocatalysis as an advanced oxidation process that can benefit from the use of solar light are highly dependent on the catalyst material that promotes the kinetics of the reactions involved. Although a huge volume of works has been published in recent years on the synthesis of new catalytic materials to be used in water remediation, which show on the one hand improved performance and on the other hand efficiency under visible light, there are still several unknown characteristics that prevent expanding the process.

In this work, we focus on a highly motivating application that addresses the degradation of the persistent pollutant perfluorooctanoic acid in aqueous matrices before it goes into the environment. To this end, a new photocatalyst composite fabricated by combining commercial P25 TiO₂ with 5% of reduced graphene oxide, which showed promising results in previous work, has been used. The influence of the working pH on the catalyst activation and the initial concentration of PFOA on the degradation kinetics have been analyzed offering new insight into the state-of-the-art. The results obtained in this work allow us to conclude the benefits of a membrane concentration step before the photocatalytic oxidation, increasing the driving force for the process kinetics.

Acknowledgments

This research was financed by the Spanish Ministry of Science, Innovation, and Universities grant number RTI2018-093310-B-I00 (MCIU/AEI/FEDER, UE) and PID2021-122563OB-I00 funded by MCIN/AEI/10.13039/501100011033/FEDER, UE.

Funding

This research did not receive any specific grant from funding agencies in the public, commercial, or not-for-profit sectors.

Declaration of Competing Interest

The authors declare that they have no known competing financial interests or personal relationships that could have appeared to influence the work reported in this paper.

CRediT authorship contribution statement

- I. Ortiz: Conceptualization; Writing - original draft; Formal analysis; Supervision.
L. Rancaño: Data curation; Investigation; Methodology; Visualization.
M.J. Rivero: Conceptualization; Validation; Writing - review & editing; Project administration; Funding acquisition.
A. Urriaga: Conceptualization; Supervision.

References

- [1] Prevedouros, K.; Cousins, I. T.; Buck, R. C.; Korzeniowski, S. H. Sources, fate and transport of perfluorocarboxylates. *Environ. Sci. Technol.* 2006, 40 (1), 32. <https://doi.org/10.1021/es0512475>
- [2] Glüge, J.; Scheringer, M.; Cousins, I. T.; Dewitt, J. C.; Goldenman, G.; Herzke, D.; Lohmann, R.; Ng, C. A.; Trier, X.; Wang, Z. An Overview of the Uses of Per- And Polyfluoroalkyl Substances (PFAS). *Environ. Sci. Process. Impacts* 2020, 22 (12), 2345. <https://doi.org/10.1039/D0EM00291G>
- [3] US Environmental Protection Agency. EPA's per- and poly-fluoroalkyl substances (PFAS) Action Plan. EPA 823R18004. Washington, DC, 2019.
- [4] Knutsen, H. K.; Alexander, J.; Barregård, L.; Bignami, M.; Brütschweiler, B.; Ceccatelli, S.; Cottrill, B.; Dinovi, M.; Edler, L.; Grasl-Kraupp, B.; Hogstrand, C.; Hoogenboom, L. (Ron); Nebbia, C. S.; Oswald, I. P.; Petersen, A.; Rose, M.; Roudot, A. C.; Vleminckx, C.; Vollmer, G.; Wallace, H.; Bodin, L.; Cravedi, J. P.; Halldorsson, T. I.; Haug, L. S.; Johansson, N.; van Loveren, H.; Gergelova, P.; Mackay, K.; Levorato, S.; van Manen, M.; Schwerdtle, T. Risk to Human Health Related to the Presence of Perfluorooctane Sulfonic Acid and Perfluorooctanoic Acid in Food. *EFSA J.* 2018, 16 (12), 5194. <https://doi.org/10.2903/j.efsa.2018.5194>
- [5] Naidu, R.; Nadebaum, P.; Fang, C.; Cousins, I.; Pennell, K.; Conder, J.; Newell, C. J.; Longpré, D.; Warner, S.; Crosbie, N. D.; Surapaneni, A.; Bekele, D.; Spiess, R.; Bradshaw, T.; Slee, D.; Liu, Y.; Qi, F.; Mallavarapu, M.; Duan, L.; McLeod, L.; Bowman, M.; Richmond, B.; Srivastava, P.; Chadalavada, S.; Umeh, A.; Biswas, B.; Barclay, A.; Simon, J.; Nathanail, P. Per- and Poly-Fluoroalkyl Substances (PFAS): Current Status and Research Needs. *Environ. Technol. Innov.* 2020, 19, 1864. <https://doi.org/10.1016/j.eti.2020.100915>
- [6] Decision SC-9/12 of the Conference of the Parties to the Stockholm Convention. Amendment to Annex A: List perfluorooctanoic acid (PFOA), its salts, and PFOA-related compounds in Annex A with specific exemptions. United Nations, 2019. Reference: C.N.588.2019.TREATIES-XXVII.15.
- [7] Wang, Z.; Cousins, I. T.; Scheringer, M.; Buck, R. C.; Hungerbühler, K. Global Emission Inventories for C4-C14 Perfluoroalkyl Carboxylic Acid (PFCA) Homologues from 1951 to 2030, Part I: Production and Emissions from Quantifiable Sources. *Environ. Int.* 2014, 70, 62. <https://doi.org/10.1016/j.envint.2014.04.013>
- [8] Fang, S.; Sha, B.; Yin, H.; Bian, Y.; Yuan, B.; Cousins, I. T. Environment Occurrence of Perfluoroalkyl Acids and Associated Human Health Risks near a Major Fluorochemical Manufacturing Park in Southwest of China. *J. Hazard. Mater.* 2020, 396, 122617. <https://doi.org/10.1016/j.jhazmat.2020.122617>
- [9] Fuertes, I.; Gómez-Lavín, S.; Elizalde, M. P.; Urriaga, A. Perfluorinated Alkyl Substances (PFASs) in Northern Spain Municipal Solid Waste Landfill Leachates. *Chemosphere* 2017, 168, 399. <https://doi.org/10.1016/j.chemosphere.2016.10.072>
- [10] Dauchy, X.; Boiteux, V.; Bach, C.; Colin, A.; Hemard, J.; Rosin, C.; Munoz, J. F. Mass Flows and Fate of Per- and Polyfluoroalkyl Substances (PFASs) in the Wastewater Treatment Plant of a Fluorochemical Manufacturing Facility. *Sci. Total Environ.* 2017, 576, 549. <https://doi.org/10.1016/j.scitotenv.2016.10.130>
- [11] Hu, X. C.; Andrews, D. Q.; Lindstrom, A. B.; Bruton, T. A.; Schaidler, L. A.; Grandjean, P.; Lohmann, R.; Carignan, C. C.; Blum, A.; Balan, S. A.; Higgins, C. P.; Sunderland, E. M. Detection of Poly- and Perfluoroalkyl Substances (PFASs) in U.S. Drinking Water Linked to Industrial Sites, Military Fire Training Areas, and Wastewater Treatment Plants. *Environ. Sci. Technol. Lett.* 2016, 3 (10), 344. <https://doi.org/10.1021/acs.estlett.6b00260>
- [12] U.S. EPA. Drinking Water Health Advisories for PFOA and PFOS. *Environ. Prot. Agency* 2016.
- [13] The European Parliament and the Council of the European Union. Directive (EU) 2020/2184, EU (Revised) Drinking Water Directive. Annex 1. Part B.

- Off. J. Eur. Communities 2020.
- [14] Schultz, M. M.; Higgins, C. P.; Huset, C. A.; Luthy, R. G.; Barofsky, D. F.; Field, J. A. Fluorochemical Mass Flows in a Municipal Wastewater Treatment Facility. *Environ. Sci. Technol.* 2006, 40 (23), 7350. <https://doi.org/10.1021/es061025m>
- [15] Yu, J.; Hu, J.; Tanaka, S.; Fujii, S. Perfluorooctane Sulfonate (PFOS) and Perfluorooctanoic Acid (PFOA) in Sewage Treatment Plants. *Water Res.* 2009, 43 (9), 2399. <https://doi.org/10.1016/j.watres.2009.03.009>
- [16] Comber, S. D. W.; Gardner, M. J.; Ellor, B. Perfluorinated Alkyl Substances: Sewage Treatment and Implications for Receiving Waters. *Sci. Total Environ.* 2021, 791, 148391. <https://doi.org/10.1016/j.scitotenv.2021.148391>
- [17] Arvaniti, O. S.; Stasinakis, A. S. Review on the Occurrence, Fate and Removal of Perfluorinated Compounds during Wastewater Treatment. *Sci. Total Environ.* 2015, 524–525, 81. <https://doi.org/10.1016/j.scitotenv.2015.04.023>
- [18] Gomez-Ruiz, B.; Gómez-Lavín, S.; Diban, N.; Boiteux, V.; Colin, A.; Dauchy, X.; Urriaga, A. Efficient Electrochemical Degradation of Poly- and Perfluoroalkyl Substances (PFASs) from the Effluents of an Industrial Wastewater Treatment Plant. *Chem. Eng. J.* 2017, 322, 196. <https://doi.org/10.1016/j.cej.2017.04.040>
- [19] Boyer, T. H.; Fang, Y.; Ellis, A.; Dietz, R.; Choi, Y. J.; Schaefer, C. E.; Higgins, C. P.; Strathmann, T. J. Anion Exchange Resin Removal of Per- and Polyfluoroalkyl Substances (PFAS) from Impacted Water: A Critical Review. *Water Res.* 2021, 200, 117244. <https://doi.org/10.1016/j.watres.2021.117244>
- [20] Soriano, Á.; Gorri, D.; Urriaga, A. Selection of High Flux Membrane for the Effective Removal of Short-Chain Perfluorocarboxylic Acids. *Ind. Eng. Chem. Res.* 2019, 58 (8), 3329. <https://doi.org/10.1021/acs.iecr.8b05506>
- [21] Wang, Z.; Su, W.; Zhang, Y. Reverse osmosis membrane design for reclamation and removal of perfluorooctanoic acid. *Desalin. Water Treat.* 2021, 237, 32. <https://doi.org/10.5004/dwt.2021.27745>
- [22] Tang, W.; Meng, Y.; Yang, B.; He, D.; Li, Y.; Li, B.; Shi, Z.; Zhao, C. Preparation of hollow-fiber nanofiltration membranes of high performance for effective removal of PFOA and high resistance to BSA fouling. *J. Environ. Sci.* 2022, 122, 14. <https://doi.org/10.1016/j.jes.2021.10.004>
- [23] Hara-Yamamura, H.; Inoue, K.; Matsumoto, T.; Honda, R.; Ninomiya, K.; Yamamura, H. Rejection of perfluorooctanoic acid (PFOA) and perfluorooctane sulfonate (PFOS) by severely chlorine damaged RO membranes with different salt rejection ratios. *Chem. Eng. J.* 2022, 446, 137398. <https://doi.org/10.1016/j.cej.2022.137398>
- [24] Olimattel, K.; Zhai, L.; Sadmani, A.H.M.A. Enhanced removal of perfluorooctane sulfonic acid and perfluorooctanoic acid via polyelectrolyte functionalized ultrafiltration membrane: Effects of membrane modification and water matrix. *J. Hazard. Mater. Letters* 2021, 2, 100043. <https://doi.org/10.1016/j.hazl.2021.100043>
- [25] Soriano, Á.; Gorri, D.; Biegler, L. T.; Urriaga, A. An Optimization Model for the Treatment of Perfluorocarboxylic Acids Considering Membrane Preconcentration and BDD Electrooxidation. *Water Res.* 2019, 164, 114954. <https://doi.org/10.1016/j.watres.2019.114954>
- [26] Soriano, A.; Schaefer, C.; Urriaga, A. Enhanced Treatment of Perfluoroalkyl Acids in Groundwater by Membrane Separation and Electrochemical Oxidation. *Chem. Eng. J. Adv.* 2020, 4, 100042. <https://doi.org/10.1016/j.cej.2020.100042>
- [27] Wang, S.; Yang, Q.; Chen, F.; Sun, J.; Luo, K.; Yao, F.; Wang, X.; Wang, D.; Li, X.; Zeng, G. Photocatalytic Degradation of Perfluorooctanoic Acid and Perfluorooctane Sulfonate in Water: A Critical Review. *Chem. Eng. J.* 2017, 328, 927. <https://doi.org/10.1016/j.cej.2017.07.076>
- [28] Liu, X.; Wei, W.; Xu, J.; Wang, D.; Song, L.; Ni, B. J. Photochemical Decomposition of Perfluorochemicals in Contaminated Water. *Water Res.* 2020, 186, 116311. <https://doi.org/10.1016/j.watres.2020.116311>
- [29] Wu, Y.; Hu, Y.; Han, M.; Ouyang, Y.; Xia, L.; Huang, X.; Hu, Z.; Li, C. Mechanism Insights into the Facet-Dependent Photocatalytic Degradation of Perfluorooctanoic Acid on BiOCl Nanosheets. *Chem. Eng. J.* 2021, 425, 130672. <https://doi.org/10.1016/j.cej.2021.130672>
- [30] Song, C.; Chen, P.; Wang, C.; Zhu, L. Photodegradation of Perfluorooctanoic Acid by Synthesized TiO₂-MWCNT Composites under 365nm UV Irradiation. *Chemosphere* 2012, 86 (8), 853. <https://doi.org/10.1016/j.chemosphere.2011.11.034>
- [31] Do, H. T.; Phan Thi, L. A.; Dao Nguyen, N. H.; Huang, C. W.; Le, Q. Van; Nguyen, V. H. Tailoring Photocatalysts and Elucidating Mechanisms of Photocatalytic Degradation of Perfluorocarboxylic Acids (PFCAs) in Water: A Comparative Overview. *J. Chem. Technol. Biotechnol.* 2020, 95 (10), 2569. <https://doi.org/10.1002/jctb.6333>
- [32] Li, F.; Wei, Z.; He, K.; Blaney, L.; Cheng, X.; Xu, T.; Liu, W.; Zhao, D. A Concentrate-and-Destroy Technique for Degradation of Perfluorooctanoic Acid in Water Using a New Adsorptive Photocatalyst. *Water Res.* 2020, 185, 1. <https://doi.org/10.1016/j.watres.2020.116219>
- [33] Zhu, C.; Xu, J.; Song, S.; Wang, J.; Li, Y.; Liu, R.; Shen, Y. TiO₂ Quantum Dots Loaded Sulfonated Graphene Aerogel for Effective Adsorption-Photocatalysis of PFOA. *Sci. Total Environ.* 2020, 698, 134275. <https://doi.org/10.1016/j.scitotenv.2019.134275>
- [34] Xu, T.; Zhu, Y.; Duan, J.; Xia, Y.; Tong, T.; Zhang, L.; Zhao, D. Enhanced Photocatalytic Degradation of Perfluorooctanoic Acid Using Carbon-Modified Bismuth Phosphate Composite: Effectiveness, Material Synergy and Roles of Carbon. *Chem. Eng. J.* 2020, 395, 124991. <https://doi.org/10.1016/j.cej.2020.124991>
- [35] Gomez-Ruiz, B.; Ribao, P.; Diban, N.; Rivero, M. J.; Ortiz, I.; Urriaga, A. Photocatalytic Degradation and Mineralization of Perfluorooctanoic Acid (PFOA) Using a Composite TiO₂-rGO Catalyst. *J. Hazard. Mater.* 2018, 344, 950. <https://doi.org/10.1016/j.jhazmat.2017.11.048>
- [36] Ribao, P.; Rivero, M. J.; Ortiz, I. TiO₂ Structures Doped with Noble Metals and/or Graphene Oxide to Improve the Photocatalytic Degradation of Dichloroacetic Acid. *Environ. Sci. Pollut. Res.* 2017, 24 (14), 12628. <https://doi.org/10.1007/s11356-016-7714-x>
- [37] Rivero, M. J.; Ribao, P.; Gomez-Ruiz, B.; Urriaga, A.; Ortiz, I. Comparative Performance of TiO₂-rGO Photocatalyst in the Degradation of Dichloroacetic and Perfluorooctanoic Acids. *Sep. Purif. Technol.* 2020, 240, 116637. <https://doi.org/10.1016/j.seppur.2020.116637>
- [38] Panchangam, S. C.; Yellatur, C. S.; Yang, J. S.; Loka, S. S.; Lin, A. Y. C.; Vemula, V. Facile Fabrication of TiO₂-Graphene Nanocomposites (TGNCs) for the Efficient Photocatalytic Oxidation of Perfluorooctanoic Acid (PFOA). *J. Environ. Chem. Eng.* 2018, 6 (5), 6359. <https://doi.org/10.1016/j.jece.2018.10.003>
- [39] Shang, E.; Li, Y.; Niu, J.; Li, S.; Zhang, G.; Wang, X. Photocatalytic Degradation of Perfluorooctanoic Acid over Pb-BiFeO₃/rGO Catalyst: Kinetics and Mechanism. *Chemosphere* 2018, 211, 34. <https://doi.org/10.1016/j.chemosphere.2018.07.130>
- [40] Park, K.; Ali, I.; Kim, J. O. Photodegradation of Perfluorooctanoic Acid by Graphene Oxide-Deposited TiO₂ Nanotube Arrays in Aqueous Phase. *J. Environ. Manage.* 2018, 218, 333. <https://doi.org/10.1016/j.jenvman.2018.04.016>
- [41] Li, J.; Zhou, S. L.; Hong, G. B.; Chang, C. T. Hydrothermal Preparation of P25-Graphene Composite with Enhanced Adsorption and Photocatalytic Degradation of Dyes. *Chem. Eng. J.* 2013, 219, 486. <https://doi.org/10.1016/j.cej.2013.01.031>
- [42] Fotiou, T.; Triantis, T. M.; Kaloudis, T.; Pastrana-Martínez, L. M.; Likodimos, V.; Falaras, P.; Silva, A. M. T.; Hiskia, A. Photocatalytic Degradation of Microcystin-LR and off-Odor Compounds in Water under UV-A and Solar Light with a Nanostructured Photocatalyst Based on Reduced Graphene Oxide-TiO₂ Composite. Identification of Intermediate Products. *Ind. Eng. Chem. Res.* 2013, 52 (39), 13991. <https://doi.org/10.1021/ie400382r>
- [43] Malekshoar, G.; Pal, K.; He, Q.; Yu, A.; Ray, A. K. Enhanced Solar Photocatalytic Degradation of Phenol with Coupled Graphene-Based Titanium Dioxide and Zinc Oxide. *Ind. Eng. Chem. Res.* 2014, 53 (49), 18824. <https://doi.org/10.1021/ie501673v>
- [44] Corredor, J.; Perez-Peña, E.; Rivero, M. J.; Ortiz, I. Performance of rGO/TiO₂ Photocatalytic Membranes for Hydrogen Production. *Membranes (Basel)* 2020, 10 (9), 1. <https://doi.org/10.3390/membranes10090218>
- [45] Martín, S. S.; Rivero, M. J.; Ortiz, I. Unravelling the Mechanisms That Drive the Performance of Photocatalytic Hydrogen Production. *Catalysts* 2020, 10 (8), 1. <https://doi.org/10.3390/catal10080901>
- [46] Chun, H. H.; Lee, J. Y.; Lee, J. H.; Jo, W. K. Enhanced Photocatalysis of Graphene and TiO₂ Dual-Coupled Carbon Nanofibers Post-Treated at Various Temperatures. *Ind. Eng. Chem. Res.* 2016, 55 (1), 45. <https://doi.org/10.1021/acs.iecr.5b02751>
- [47] Jo, W. K.; Tayade, R. J. New Generation Energy-Efficient Light Source for Photocatalysis: LEDs for Environmental Applications. *Ind. Eng. Chem. Res.* 2014, 53 (6), 2073. <https://doi.org/10.1021/ie404176g>
- [48] Domínguez, S.; Rivero, M. J.; Gomez, P.; Ibañez, R.; Ortiz, I. Kinetic modeling and energy evaluation of sodium dodecylbenzene sulfonate photocatalytic degradation in a new LED reactor. *J. Ind. Eng. Chem.* 2016, 37, 237. <https://doi.org/10.1016/j.jiec.2016.03.031>
- [49] Ranaño, L.; Rivero, M. J.; Mueses, M. Á.; Ortiz, I. Comprehensive Kinetics of the Photocatalytic Degradation of Emerging Pollutants in a Led-Assisted Photoreactor. S-Metolachlor as Case Study. *Catalysts* 2021, 11 (1), 1. <https://doi.org/10.3390/catal11010048>
- [50] Ochiai, T.; Iizuka, Y.; Nakata, K.; Murakami, T.; Tryk, D. A.; Koide, Y.; Morito, Y.; Fujishima, A. Efficient Decomposition of Perfluorocarboxylic Acids in Aqueous Suspensions of a TiO₂ Photocatalyst with Medium-Pressure Ultraviolet Lamp Irradiation under Atmospheric Pressure. *Ind. Eng. Chem. Res.* 2011, 50 (19), 10943. <https://doi.org/10.1021/ie1017496>

- [51] Federation, W. E. Standard Methods for the Examination of Water and Wastewater. Public Health 1999, 51 (1), 940.
- [52] Ribao, P.; Coreodor, J.; Rivero, M. J.; Ortiz, I. Role of Reactive Oxygen Species on the Activity of Noble Metal-Doped TiO₂ Photocatalysts. *J. Hazard. Mater.* 2019, 372, 45. <https://doi.org/10.1016/j.jhazmat.2018.05.026>
- [53] Sansotera, M.; Persico, F.; Pirola, C.; Navarrini, W.; Di Michele, A.; Bianchi, C. L. Decomposition of Perfluorooctanoic Acid Photocatalyzed by Titanium Dioxide: Chemical Modification of the Catalyst Surface Induced by Fluoride Ions. *Appl. Catal. B Environ.* 2014, 148–149, 29. <https://doi.org/10.1016/j.apcatb.2013.10.038>
- [54] Wang, W. N.; Jiang, Y.; Fortner, J. D.; Biswas, P. Nanostructured Graphene-Titanium Dioxide Composites Synthesized by a Single-Step Aerosol Process for Photoreduction of Carbon Dioxide. *Environ. Eng. Sci.* 2014, 31 (7), 428. <https://doi.org/10.1089/ees.2013.0473>
- [55] Yao, X.; Zuo, J.; Wang, Y.-J.; Song, N.-N.; Li, H.-H.; Qiu, K. Enhanced Photocatalytic Degradation of Perfluorooctanoic Acid by Mesoporous Sb₂O₃/TiO₂ Heterojunctions. *Front. Chem.* 2021, 9, 1. <https://doi.org/10.3389/fchem.2021.690520>
- [56] Panchangam, S. C.; Lin, A. Y. C.; Shaik, K. L.; Lin, C. F. Decomposition of Perfluorocarboxylic Acids (PFCAs) by Heterogeneous Photocatalysis in Acidic Aqueous Medium. *Chemosphere* 2009, 77 (2), <https://doi.org/10.1016/j.chemosphere.2009.07.003>
- [57] Dillert, R.; Bahnemann, D.; Hidaka, H. Light-Induced Degradation of Perfluorocarboxylic Acids in the Presence of Titanium Dioxide. *Chemosphere* 2007, 67 (4), 785. <https://doi.org/10.1016/j.chemosphere.2006.10.023>
- [58] Xu, B.; Ahmed, M. B.; Zhou, J. L.; Altaee, A. Visible and UV Photocatalysis of Aqueous Perfluorooctanoic Acid by TiO₂ and Peroxymonosulfate: Process Kinetics and Mechanistic Insights. *Chemosphere* 2020, 243, 125366. <https://doi.org/10.1016/j.chemosphere.2019.125366>
- [59] Chen, M. J.; Lo, S. L.; Lee, Y. C.; Kuo, J.; Wu, C. H. Decomposition of Perfluorooctanoic Acid by Ultraviolet Light Irradiation with Pb-Modified Titanium Dioxide. *J. Hazard. Mater.* 2016, 303, 111. <https://doi.org/10.1016/j.jhazmat.2015.10.01>
- [60] Vierke, L.; Berger, U.; Cousins, I. T. Estimation of the Acid Dissociation Constant of Perfluoroalkyl Carboxylic Acids through an Experimental Investigation of Their Water-to-Air Transport. *Environ. Sci. Technol.* 2013, 47 (19), 11032. <https://doi.org/10.1021/es402691z>
- [61] López-Fontán, J. L.; Sarmiento, F.; Schulz, P. C. The Aggregation of Sodium Perfluorooctanoate in Water. *Colloid Polym. Sci.* 2005, 283 (8), 862. <https://doi.org/10.1007/s00396-004-1228-7>
- [62] Cheng, J.; Psillakis, E.; Hoffmann, M. R.; Colussi, A. J. Acid Dissociation versus Molecular Association of Perfluoroalkyl Oxoacids: Environmental Implications. *J. Phys. Chem. A* 2009, 113 (29), 8152. <https://doi.org/10.1021/jp9051352>
- [63] Burns, D. C.; Ellis, D. a.; Li, H.; Memundo, C. J.; Webster, E. Comment on “Experimental PK_a Determination for Perfluorooctanoic Acid (PFOA) and the Potential Impact of PK_a Concentration Dependence on Laboratory-Measured Partitioning Phenomena and Environmental Modeling.” *Environ. Sci. Technol.* 2009, 43 (13), 5150. <https://doi.org/10.1021/es900451s>